

# Numerical Parametric Study on Full Coverage Cooled Multi-Layer Plates

Dieter BOHN and Norbert MORITZ

Institute of Steam and Gas Turbines  
Aachen University

Templergraben 55, D-52056 Aachen, GERMANY

Phone: +49-241-8025451, FAX: +49-241-8022307, E-mail: post-bohn@idg.rwth-aachen.de

## ABSTRACT

A full-coverage cooled multi-layer plate configuration is investigated numerically by application of a 3-D conjugate fluid flow and heat transfer solver, CHTflow. The geometrical setup and the fluid flow conditions are derived from modern gas turbine combustion chambers and bladings.

The numerical grid contains the coolant supply (plenum), the solid body, and the main flow area upon the plate. The full-coverage cooling is realized by finest drilled holes with a diameter of 0.2 mm that are shaped in the region of the thermal barrier coating. The holes are inclined with an angle of 30°. Two different configurations are investigated that differ in the shaping of the holes in their outlet region.

The numerical investigation focusses on the influence of hot gas mass flow and blowing ratio on the cooling film development and the local heat flux and cooling efficiency on the plate surface and on the cooling hole surface.

## NOMENCLATURE

B	[ m ]	hole shaping parameter
D	[ m ]	hole diameter
H	[ m ]	lateral distance of cooling holes
L	[ m ]	distance of rows of cooling holes
M	[ - ]	blowing ratio
Ma	[ - ]	Mach number
T	[ K ]	temperature
p	[ N/m <sup>2</sup> ]	pressure
q	[ W ]	heat flux
v	[ m/s ]	velocity
x, y, z	[ m ]	Cartesian coordinate
$\alpha$	[ ° ]	angle of inclination
$\beta_1, \beta_2$	[ ° ]	hole shaping parameters
$\rho$	[ kg/m <sup>3</sup> ]	density
$\eta$	[ - ]	efficiency

## Subscripts

b	bearable
C	cooling fluid conditions
c	cooling
H	hot gas conditions
max	maximum
min	minimum
st	static

sub	substrate
t	total
1	at inlet
2	at exit
<b>Superscripts</b>	
"	areal
-	averaged

## INTRODUCTION

Increasing the efficiency of modern gas turbines is still an important object of scientific research. One of the most important issues is the improvement of cooling technology both in the combustion chamber and in the vanes and blades of the turbine. Film cooling configurations have been investigated for several years. Concerning the CFD research in this subject, a bibliography (1971-1996) of the most important publications can be found in a study by Kercher (1998). Former numerical investigations focus on the development of the kidney vortices (Bergeles et al., 1978) in the case of flat plate cooling with one ejection hole. A detailed numerical analysis of the film cooling physics in the case of a flat plate with one row of cooling holes has been carried out by McGovern and Lylek (1997). Those test cases are investigated by an aerothermal analysis of the fluid flow. The influence of heat conduction in the solid body is neglected. Recently, the physical phenomena of leading edge film cooling were investigated experimentally and numerically by York and Lylek (2000a, 2000b).

Numerical investigations of entire blades with film cooling configurations have been presented by Garg (1999) and by Heidmann et al. (1999). These investigations show the aerothermal effects of the cooling fluid flow on the main flow field without consideration of the influence of heat transfer in the solid body.

In experimental and numerical analysis, Fottner and Ganzert (2000) investigated the flow field injections through inclined shaped holes in a cascade test tunnel. Here, the numerical investigations neglect the influence of the solid body, too. Although the numerical results show a large zone of recirculation in the cooling holes a good cooling configuration is stated. The accuracy of the results should be reviewed by application of a different numerical method with consideration of heat transfer in the solid body.

## GEOMETRIC CONFIGURATION

In this analysis a multi-layer flat plate composed of three materials is investigated. The substrate layer is of the super alloy

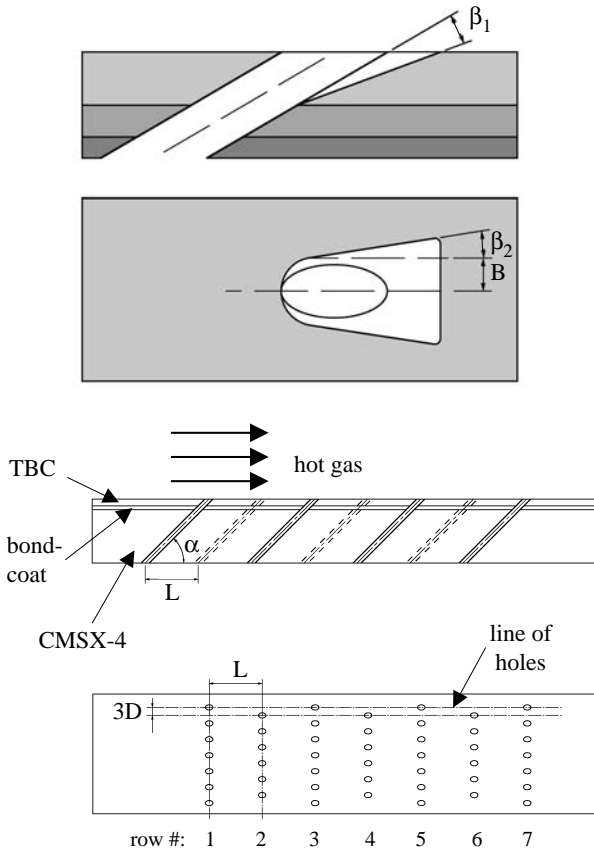


Fig. 1 Geometry of the investigated plate

CMSX-4 and has a thickness of 2,0 mm (fig. 1). The bondcoat consists of a MCrAlY layer with a thickness of 0,15 mm. The thermal barrier coating (TBC) is a Yttrium stabilized ZrO<sub>2</sub> layer with 0,25 mm thickness.

The plate is perforated with seven rows of staggered cooling holes each with a diameter of  $D=0,2$  mm. The distance between two rows of holes is  $L=6D$ , the lines of holes have a distance of  $H=3D$ . Two different cooling configurations are investigated that vary the shaping of the outlet region of the cooling holes. The shaping is applied only in the region of the thermal barrier coating, the main parameters can be found on table 1. The configuration S30-06-F has a diffuser that expands the outlet area of the cooling holes mainly in the direction of the hot gas flow on the downstream edge of the holes. Additionally, for configuration S30-06-FL the outlet diffuser is widened in lateral direction to increase the outlet area.

The conjugate analysis of the complete film cooling problem

Table 2: Main boundary conditions

	$Ma_H$	0,10		0,25	
		M	0,28	0,48	0,28
$p_{1,t}$	[MPa]	2,01252	2,01252	2,11213	2,11213
$T_{1,t}$	[K]	1575,93	1575,93	1598,34	1598,34
$p_{2,st}$	[MPa]	1,9984	1,9984	1,9984	1,9984
$p_{C,t}$	[MPa]	2,004	2,008	2,023	20,55
$T_{C,t}$	[K]	723,15	723,15	723,15	723,15

Table 1 Parameters of the investigated configurations

configuration	L	$\alpha$	$\beta_1$	$\beta_2$	B
S30-06-P-F	6D	30°	8°	0°	0,6088 D
S30-06-P-FL	6D	30°	8°	10°	0,6088 D

requires a high amount of computational time due to the necessity of high resolution grid that can compute the heat transfer into the solid body with a sufficient accuracy. In the case of leading edge ejection the authors have shown that the influence of the solid body on the flow field is not negligible to calculate the surface temperature distribution of blades. In former publications the authors have proved that the conjugate method is an excellent tool for the design process of multi-layer cooling configurations (Bohn and Moritz, 2000a).

## NUMERICAL METHOD

The numerical scheme of the code works on the basis of an implicit finite volume method combined with a multi-block technique. The physical domain is divided into separate blocks and the full, compressible, three-dimensional Navier-Stokes equations are solved in the fluid blocks. The governing equations for the conservative variables are formulated in arbitrary, body-fitted coordinates in order to allow the simulation of complex geometries. The conservation equations are discretized implicitly to the first order in time making use of the Newton method (Schmatz, 1988). Upwind discretization is used for the inviscid fluxes (Eberle et al., 1990). The viscous fluxes are approximated using central differences. The resulting system of linear equations is solved by a Gauss-Seidel point iteration scheme, allowing high vectorization on present day computers.

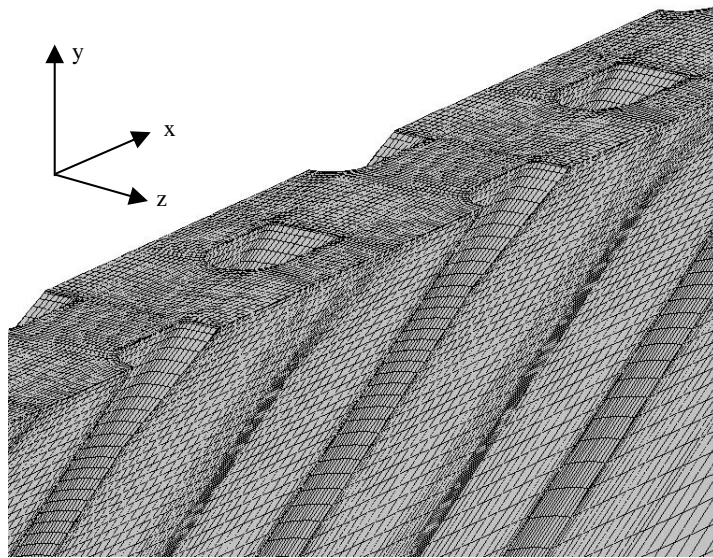
In the solid body region, the system of the governing equations is reduced to the Fourier equation. This equation is solved directly being coupled to the fluid flow region. The coupling of fluid blocks and solid body blocks is achieved via a common wall temperature, resulting from the equality of the local heat fluxes passing through the contacting cell faces. A more detailed description of the conjugate calculation method and its validation can be found in Bohn et al. (1995a, 1995b).

For the closure of the conservation equations the algebraic eddy-viscosity turbulence model by Baldwin and Lomax (1978) is used.

## COMPUTATIONAL GRID, BOUNDARY CONDITIONS AND CONVERGENCY

Fig. 2 shows an example of the numerical grid in the solid region of configuration S30-06-F. In total, it consists of 138 blocks (solid region and fluid flow) with approximately 1.800.000 points. The conjugate approach requires a high grid resolution in the boundary layers so that in the area of the cooling holes three concentrically arranged O-type blocks are used. To reduce the numerical effort only the area between the center lines of two lines of rows are investigated. At the z-planes through to the middle axis of the holes a symmetry boundary condition is used.

The inlet and outlet boundary conditions are specified as sketched on the right-hand side in fig. 2. In a distance of 5 mm from the plate surface a adiabatic wall boundary condition is set. The inlet of the plenum has a distance of 2 mm from the bottom of the plate. On the left-hand side and the right-hand side of the plenum a adiabatic wall boundary condition is set. For both



**configuration S30-06-F and S30-06-FL:**

- 138 blocks
- 1 800 000 points

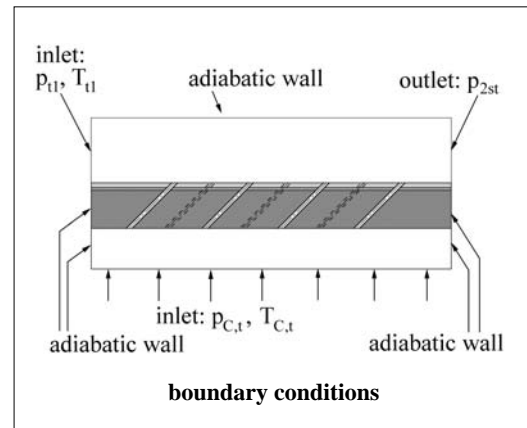


Fig. 2 Computational grid (configuration S30-06-F) and boundary conditions

configuration S30-06-F and configuration S30-06-FL four different flow conditions were analyzed. By adjusting the total pressure and total temperature at the hot gas inlet boundary the Ma number in the hot gas was set to  $Ma_H=0,1$  and  $Ma_H=0,25$ . Especially the lower Ma number represents the flow conditions in modern gas turbine combustion chambers. As this type of full-coverage cooling configuration should be applicable to gas turbine bladings, too, in a first step the hot gas Ma number of 0,25 was chosen. For each Ma number two different blowing ratios M were analyzed. The blowing ratio M is defined as

$$M = \frac{(\overline{\rho \cdot v})_C}{(\overline{\rho \cdot v})_H} \quad (1)$$

with density  $\rho$  and the velocity  $v$ . The values of the blowing ratio ( $M=0,28$  and  $M=0,48$ ) were adjusted by changing the total pressure of the cooling fluid inlet boundary.

The calculations were performed on a SUNfire workstation cluster at the computational center of Aachen University. Each computation was subdivided into 9 tasks performing the data transfer using the MPI library. As the convergency criterion the behaviour of the solid temperatures in the vicinity of the fourth row of cooling holes was used. This is necessary because the change in residuals of the solid materials is very small even if the change in temperature is significant. The computations were assumed to be converged when in 2 subsequent runs of each 5000 timesteps the change of temperature at the interfaces plenum/substrate, substrate/bondcoat, bondcoat/TBC and TBC/main flow was lower than 0,5 K.

**RESULTS**

The aim of this investigation is to provide a geometric setup for full-coverage cooling configurations that cools the substrate layer sufficiently in the case of an application in modern gas turbines. The scientific work is embedded in a Collaborative Research Center at Aachen University. The geometries presented in this paper are realized by laser drilling.

**Cooling film structure**

The reduction of the cooling fluid mass flow that is necessary to cool the substrate layer sufficiently demands the development of a homogeneous cooling film on the plate. This leads to an increase of cooling efficiency as the authors have shown in former publications (Bohn and Moritz, 2000a, 2000b). These investigations showed that the development of the kidney vortices that are induced by the interaction of cooling fluid and hot gas flow can be eliminated. These investigations did not take into account the plenum so that the kidney vortex system that is generated in the inclined cooling holes ( $\Omega_0$  structure), was not contained in the flow field.

By application of the hole shaping at the outlet side of the cooling holes the development and distribution of the  $\Omega_0$  structure can be influenced significantly. In fig. 3 the structure of the cooling film downstream the fourth row of cooling holes is shown. Due to the application of symmetry boundary conditions at the middle axes of the staggered holes the numerical domain has been mirrored at one symmetry line to show the entire cooling jet of one cooling hole. A 2D cutting plane that is perpendicular to the hot gas flow direction and the plate surface was placed close to fourth cooling hole as sketched at the bottom of fig. 3.

The pictures show the temperature distribution and the secondary flow vectors in the cooling film. The lower edge of each picture coincides with the plate surface. The temperature grey scale scheme is given at the bottom of fig. 3. Velocity vectors are scaled by the same value for each picture.

For all configurations and flow conditions it can be stated that a homogeneous cooling is found on the plate surface, i. e., the plate surface has no contact to the hot gas. Increasing the blowing ratio leads to an increase of the thermal boundary layer and additionally an expansion of the cooling jet in lateral direction. The lateral extension of the hole shaping in configuration S30-06-FL leads to a widening of the cooling jet, too, and thus to a decreased surface temperature.

The secondary flow vectors show that the elimination of the  $\Omega_0$  structure cannot be achieved with these geometric configurations.

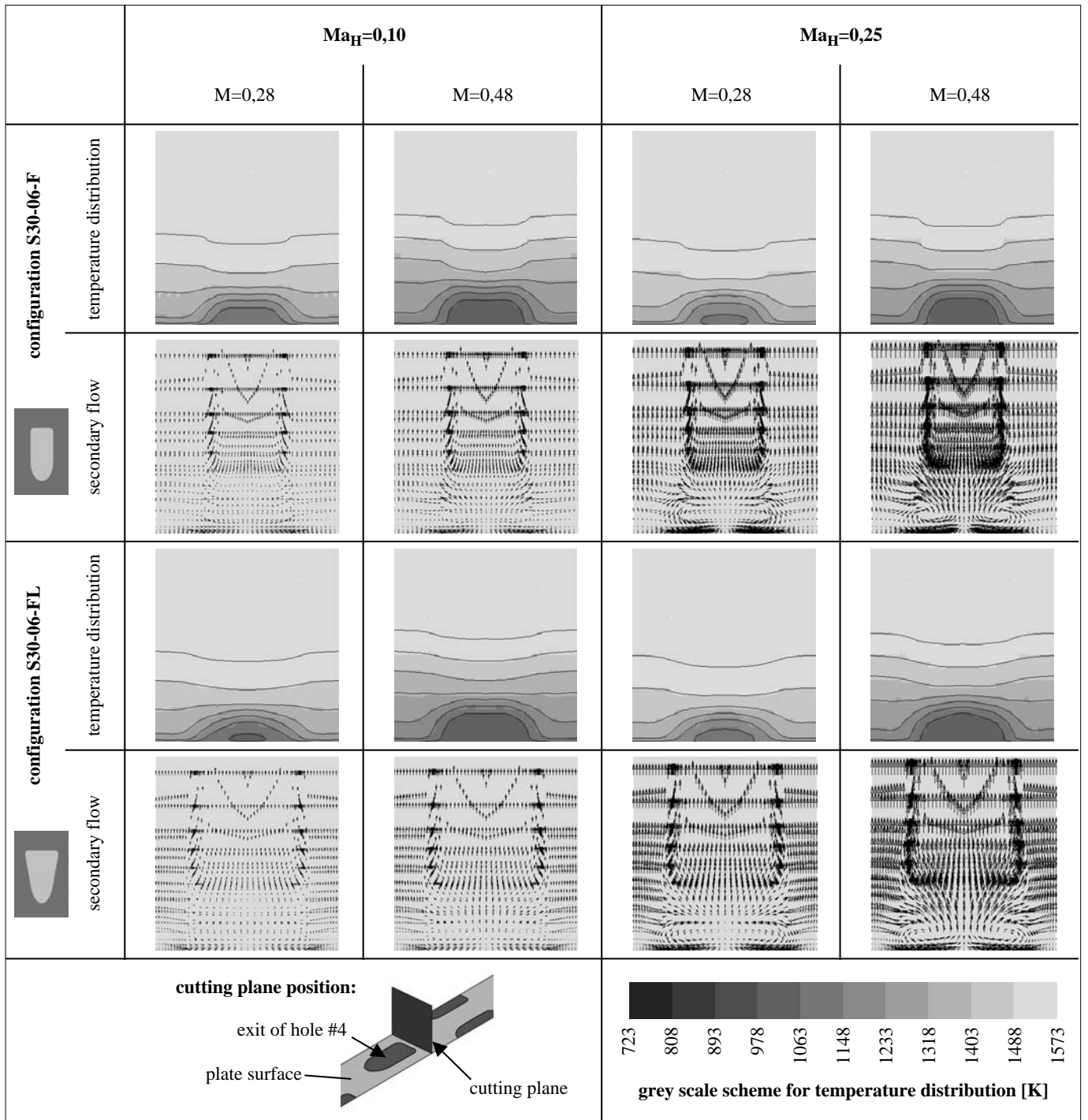


Fig. 3 Temperature distribution and secondary flow in cooling film

In the case of the low hot gas  $Ma_H=0,1$  very weak kidney vortices can be detected. The increase of the hot gas  $Ma$  number to  $Ma_H=0,25$  leads for identical blowing ratio compared to the lower  $Ma$  number to higher velocities in the cooling holes. Thus, stronger kidney vortices are generated in the cooling holes by an enlargement of the well-known separation zone at the hole inlet (e. g. Bohn and Kusterer, 1998). These vortex systems can be detected clearly in the pictures on the right hand side of fig. 3. It can be seen that the cores of the kidney vortices that are generated by hole #4 are disposed in lateral direction from the middle axis of the hole in the case of configuration S30-06-FL. For all flow

conditions it can be stated that the kidney vortex systems of the preceding rows of cooling holes are diminished at this position.

#### Analysis on plate surface

Fig. 4 shows pictures of the plate surface in the area between the downstream edge of hole #3 and the upstream edge of hole #5. On the left hand side the distribution of the cooling efficiency that is defined as

$$\eta_c = \frac{T - T_H}{T_C - T_H} \quad (2)$$

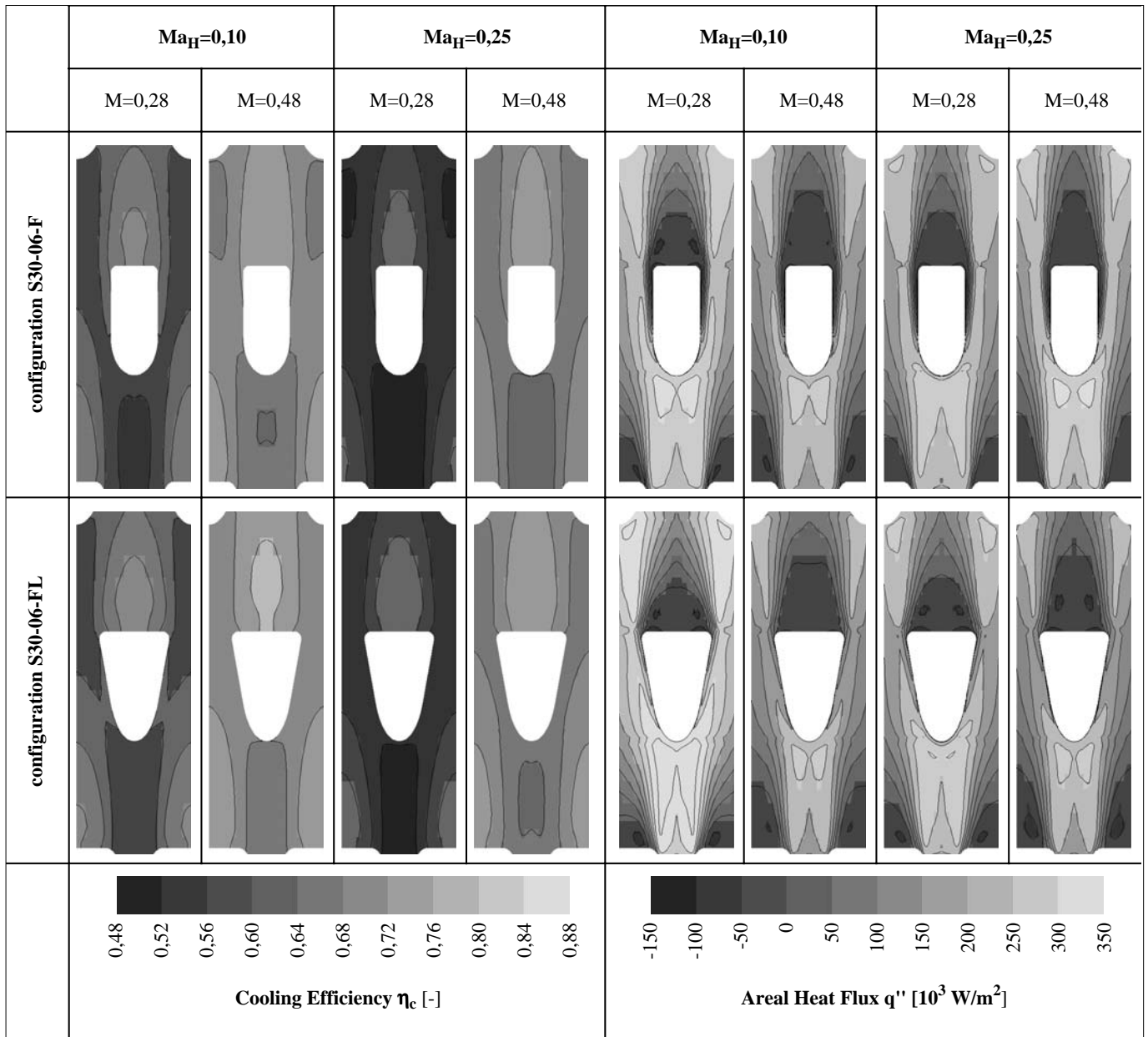


Fig. 4 Cooling efficiency and areal heat flux distribution on plate surface

is displayed. Here,  $T$  is the local surface temperature,  $T_H$  is the static hot gas temperature and  $T_C$  indicates the static cooling fluid temperature.

On the right hand side the distribution of the areal heat flux  $q''$  is shown. Negative values indicate the regions where heat is conducted from the solid into the fluid and positive values represent the regions where the solid is heated by the fluid.

The distribution of the cooling efficiency  $\eta_c$  shows that the increase of the hot gas  $Ma$  number reduces the cooling efficiency significantly for identical blowing ratios. This is caused by the higher velocity in the hot gas flow which increases the average heat transfer into the solid body. Regarding the most efficiently cooled area downstream the fourth cooling hole it can be seen that the lateral widening of the hole shaping in configuration S30-06-FL has two effects. The cooled area is increased in lateral direction. Beyond that it is extended in the direction of the hot gas flow direction. Thus, an increased protection of the plate surface

can be stated.

For configuration S30-06-FL the most efficiently cooled area is located downstream from the cooling hole, whereas for configuration S30-06-F an extension of this area in upstream direction beside the cooling hole can be detected. This can be explained by the additional angle  $\beta_2$  for configuration S30-06-FL that leads to a modification of the interaction of the outflowing cooling fluid and the hot gas at the lateral edges of the cooling holes.

This effect can be seen in the areal heat flux distribution, too. The zone with negative heat fluxes reaches some distance upstream in case of configuration S30-06-F. This indicates that the lateral edges of the cooling holes are protected by cooling fluid in this region. For configuration S30-06-FL the hot gas flow seems to reach the lateral hole edge so that only the influence of convection cooling can be seen here.

On the other hand, the negative heat flux area downstream the

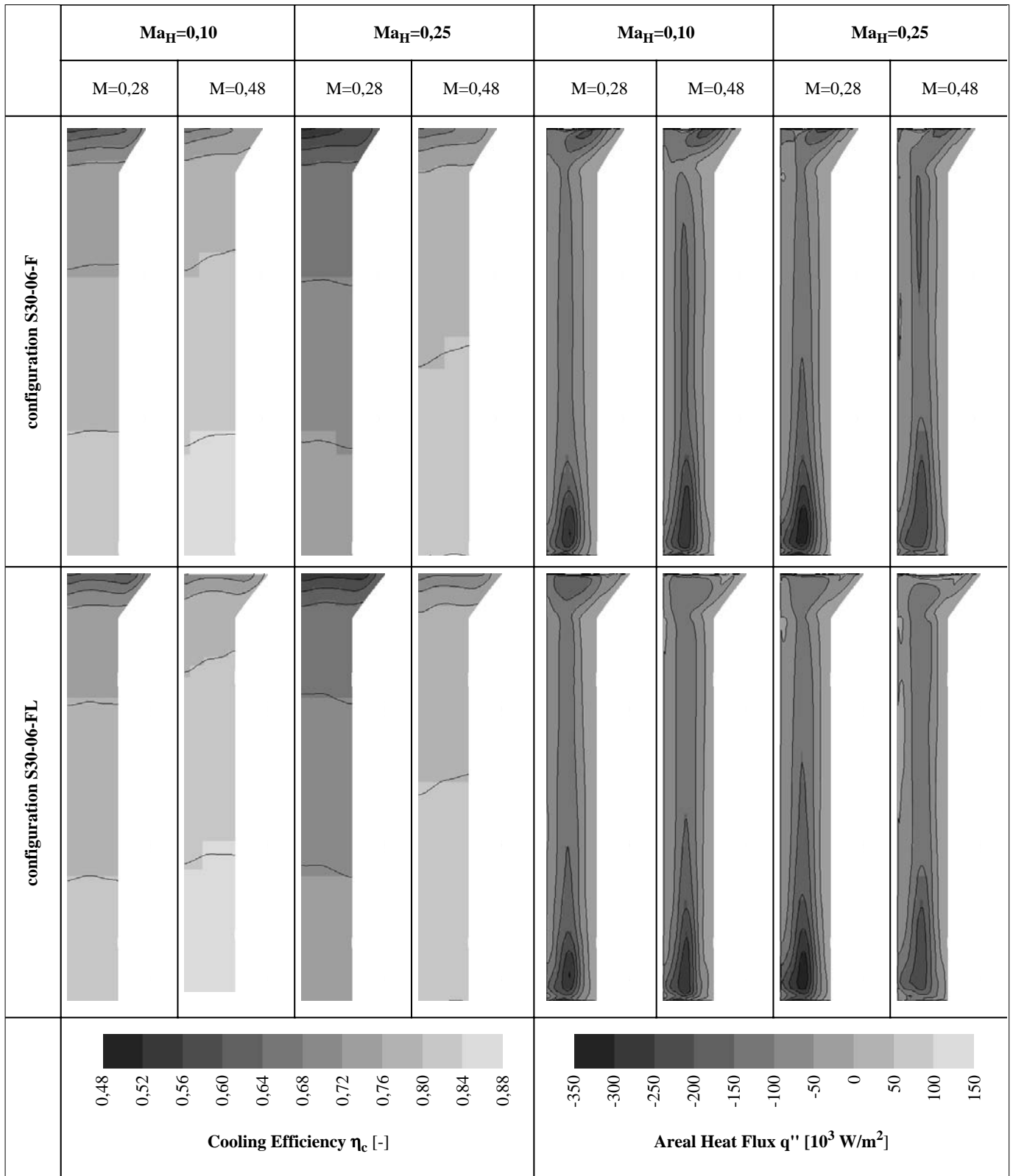


Fig. 5 Cooling efficiency and areal heat flux distribution on cooling hole surface

cooling hole is increased significantly for configuration S30-06-FL which leads, aided by the reduction of the area with positive heat fluxes, to the increased over all cooling efficiency for configuration S30-06-FL. In a next step it should be investigated whether it is possible to combine the benefits of the two geometries in an improved configuration.

#### Analysis of hole surface

In Fig. 5 the distribution of the cooling efficiency  $\eta_c$  and the areal heat flux on surface of the fourth cooling hole is depicted. The surface of one half cooling hole is displayed as a 2D plane and the middle axis that is inclined by an angle of  $\alpha=30^\circ$  is turned in vertical direction. The cooling fluid enters the cooling hole at

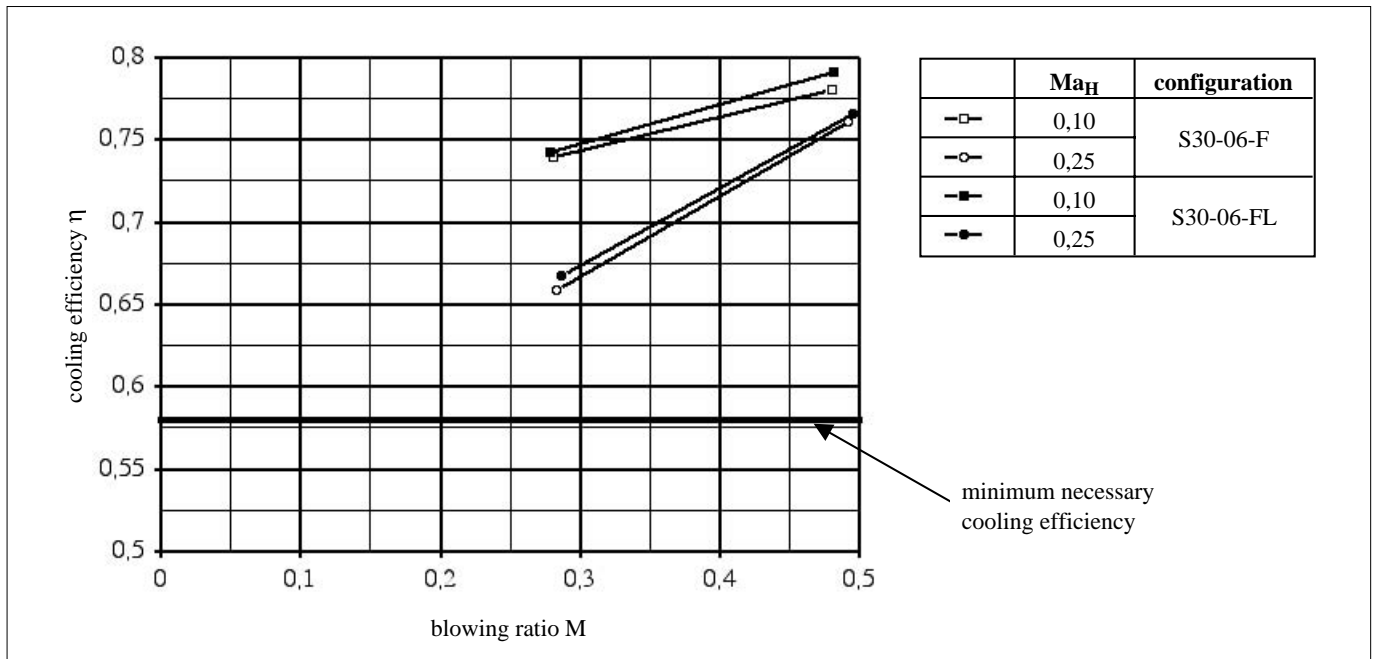


Fig. 6 Minimum cooling efficiency in substrate layer

the lower edge of the pictures. The left edge of the pictures is the upstream edge of the cooling hole that is located in the symmetry plane through the middle axes of the cooling holes #2, #4 and #6. The definitions of cooling efficiency and areal heat flux are the same as explained for the plate surface analysis.

In the zone of the cylindrical shape of the cooling hole only a small influence of the differences of the hole shaping can be detected. The cooling efficiency is decreasing from the hole inlet to the boundary between bondcoat and thermal barrier coating nearly linearly. In the region of the shaping the analysis of the different interaction of the hot gas flow and the cooling fluid flow at the lateral outlet edges of the hole are proved. The zone of reduced cooling efficiency at this edge is increased for configuration S30-06-FL. Due to the low heat conductivity of the thermal barrier coating and the increased average cooling efficiency on the plate surface this effect leads not to higher temperatures and, thus, lower cooling efficiencies in the substrate layer. On the contrary, the substrate layer is cooled more efficiently for configuration S30-06-FL.

The areal heat flux distribution shows that nearly in the entire cooling hole the heat is transported from the solid body into the cooling fluid. The exception can be detected near to the lateral outlet edge of the hole especially in the case of configuration S30-06-FL. The highest heat transfer into the cooling fluid can be found near the inlet of the hole. This is induced by the high velocities in inner part of the inlet area that are caused by the separation of the flow at the downstream side of the hole inlet edge. The influence of the shaping on the heat flux distribution in the cylindrical part of the holes is small.

An improvement of the flow structure in the cooling holes could be achieved by a modification of the inlet edge of the hole by application of a radius. This improvement was not taken into account because this full-coverage cooling configuration shall be applicable not only in combustion chambers but also in gas turbine bladings.

#### Cooling efficiency in substrate layer

The evaluation of the quality of the cooling configurations can be performed by analysis of the cooling efficiency of the substrate layer. This metallic layer, though it is a superalloy, can bear the lowest temperature of the three materials in this multi-layer structure. The highest bearable substrate temperature can be assumed to  $T_b=1173$  K.

Therefore the maximum substrate temperature in the vicinity of hole #4 was detected and the corresponding cooling efficiency for this temperature determined (eq. (2)). Fig. 6 shows the graphs for the two cooling configurations and the two hot gas  $Ma$  numbers. It can be seen that configuration S30-06-FL has a higher cooling efficiency for the investigated blowing ratios. The decrease of cooling efficiency for the lower blowing ratio is significantly higher for  $Ma_H=0,25$ . Here an additional investigation of the heat fluxes in the solid body is necessary to explain this effect.

In another project of the Collaborative Research Center a cycle analysis of a entire combined cycle power plant is performed to evaluate the contribution of each project to the aim of rising the thermal efficiency of the power plant by application of innovative cooling technologies and materials. One result of this project are the thermodynamic conditions of the hot gas at the gas turbine inlet and cooling fluid temperatures. Here, a hot gas temperature  $T_H=1593$  K and a cooling fluid temperature of  $T_C=693$  K are predicted at the present state of work to achieve a maximum thermal efficiency. With these values a minimum cooling efficiency of  $\eta_c=0,579$  can be determined that has to be reached by the full-coverage cooling. It can be seen in fig. 6 that this minimum value is exceeded for all investigated configurations.

Thus, in further investigations the minimum cooling fluid mass flow will be determined by reducing the blowing ratio. Additionally, the hot gas  $Ma$  number will be increased.

## CONCLUSIONS

A numerical conjugate flow and heat transfer analysis has been applied to a flat plate with full-coverage cooling configurations. The flow conditions were derived from modern gas turbine combustion chambers and bladings.

The influence of hot gas Ma number and blowing ratio on the cooling film structure, the cooling efficiency and the local surface heat fluxes has been investigated.

The analysis shows that the lateral widening of the shaping leads to an increase of the mean cooling efficiency and the mean heat fluxes on the plate surface. In the close vicinity of the lateral outlet edges of the cooling holes an increase of the thermal load can be detected. This is induced by the interaction of the hot gas flow and the ejecting cooling fluid.

In the cylindrical part of the cooling holes only small influences of the different hole shaping on the cooling efficiency and the heat fluxes can be detected. The heat flux distribution is dominated by cooling hole inlet flow structures, i. e. the separation zone which induced the kidney vortices in the hole.

For the investigated blowing ratio it can be stated that the substrate layer is cooled sufficiently for both cooling configurations. In further investigations the minimum cooling fluid mass flow can be determined which still provides a sufficient cooling efficiency by reduction of the blowing ratio.

Additionally, the geometry of the hole shaping shall be modified to obtain a cooling configuration that combines the benefits of the two investigated configurations. Another aim is to extend the lateral hole distance so that real gas turbine components can be cooled with a lower number of cooling holes.

## ACKNOWLEDGEMENTS

The authors gratefully acknowledge the financial support of the Deutsche Forschungsgemeinschaft (DFG) within the Collaborative Research Center (SFB) 561 "Thermally Highly Loaded, Porous and Cooled Multi-Layer Systems for Combined Cycle Power Plants". The responsibility for the content of this publication lies upon the authors.

## REFERENCES

- Baldwin, B. S., and Lomax, H., 1978, "Thin Layer Approximation and Algebraic Model for Separated Turbulent Flows", *AIAA-paper 78-257*
- Bergeles, G., Gosman, A.D., and Launder, B.E., 1976, "The Prediction of Three-Dimensional Discrete-Hole Cooling Processes", *Journal of Heat Transfer*, 98, pp. 379-386
- Bohn, D., Bonhoff, B., Schönenborn, H., Wilhelmi, H., 1995a, "Validation of a Numerical Model for the Coupled Simulation of Fluid Flow and Diabatic Walls with Application to Film-cooled Turbine Blades", *VDI-Berichte 1186*
- Bohn, D., Schönenborn, H., Bonhoff, B. and Wilhelmi, H., 1995b, "Prediction of the Film-cooling Effectiveness in Gas Turbine Blades Using a Numerical Model for the Coupled Simulation of Fluid Flow and Diabatic Walls", *ISABE 95-7105*
- Bohn, D. and Kusterer, K., "3D Numerical Aerodynamic and Combined Heat Transfer Analysis of a Turbine Guide Vane with Showerhead Ejection", *Heat Transfer 1998, Proceedings of 11 th IHTC*, Vol.4 , pp. 313-318, Kyongju, Korea, August 1998

Bohn, D., and Moritz, N., 2000a, "Influence of Hole Shaping of Staggered Multi-Hole Configurations on Cooling Film Development", *AIAA-paper 2000-2579*

Bohn, D., and Moritz, N., 2000b, "Influence of Blowing Ratio on the Thermal Load of Transpiration Cooled Flat Plates", *2nd Int. Symp. on Fluid Machinery and Fluid Engineering*, Beijing, China, October 2000

Eberle, A., Schmatz, M.A., and Bissinger, N., 1990, "Generalized Flux Vectors for Hypersonic Shock-Capturing", *AIAA-paper 90-0390*

Grag, V.K., 1999, "Heat Transfer on a Film-Cooled Rotating Blade", *ASME 99-GT-44*

Fottner, L., and Ganzert, W., "Aerodynamische Optimierung der Kühlluft-Ausblasekonfigurationen fortschrittlicher Turbinenbeschauelungen", *Informationstagung der FVV*, spring 2000, Frankfurt a. M.

Heidmann, J.D., Rigby, D.L., and Ameri, A.A., 1999, "A 3D Coupled Internal/External Simulation of a Film-Cooled Gas Turbine", *ASME 99-GT-186*

Kercher, D. M., 1998, "A Film-Cooling CFD Bibliography: 1971-1996", *Int. Journ. of Rot. Mach.*, 4 No. 1, pp. 61-72

McGovern, K.T., and Leylek, J.H., 1997, "A Detailed Analysis of Film Cooling Physics Part II. Compound-Angle Injection with Cylindrical Holes", *ASME 97-GT-270*

Grag, V.K., 1999, "Heat Transfer on a Film-Cooled Rotating Blade", *ASME 99-GT-44*

Schmatz, M.A., 1988, "Three-dimensional Viscous Flow Simulations Using an Implicit Relaxation Scheme", *Notes on Numerical Fluid-Mechanics (NNFM)*, 22, Vieweg, Braunschweig, pp. 226-242

York, W.D., and Leylek, J.H., 2002a, "Leading Edge Film-Cooling Physics: Part I - Adiabatic Effectiveness", *ASME GT-2002-30166*

York, W.D., and Leylek, J.H., 2002b, "Leading Edge Film-Cooling Physics: Part II - Heat Transfer Coefficient", *ASME GT-2002-30167*